

Base-isolated building with high-damping spring system subjected to near fault earthquakes

Miguel Eduardo Tornello*¹ and Mauricio Sarrazin²

¹*Regional Center of Technological Developments for Construction, Seismology and Earthquake Engineering (CeReDeTec.), National Technological University, Rodriguez 273 (5500), Mendoza, Argentina*

²*Department of Civil Engineering, University of Chile, Beauchef 850, Santiago (8370448), Chile*

(Received March 18, 2011, Revised March 10, 2012, Accepted April 10, 2012)

Abstract. There are many types of seismic isolation devices that are being used today for structural control of earthquake response in buildings. The most commonly used are sliding bearings and elastomeric bearings, the latter with or without lead core. An alternative solution is the use of steel springs combined with viscoelastic fluid dampers, which is the case discussed in this paper. An analytical study of a three-story building supported on helical steel springs and viscoelastic fluid dampers, GERB Control System (GCS), subjected to near-fault earthquakes is presented. Several earthquakes records have been obtained by the acceleration network installed in the isolated building and in its non-isolated twin since they were finished. These experimental results are analysed and discussed. The aim is to show that the spring-based system can be an alternative for base isolation of small building located near active faults.

Keywords: building base isolation; spring bearing; viscous damping; near fault earthquakes

1. Introduction

Base-isolation devices allow us to reduce seismic demands on structures by filtering the seismic waves and dissipating energy at well controlled and specially designed elements, thus improving their capacity to overpass destructive earthquakes. The most commonly used isolators are sliding bearings and elastomeric bearings, with or without lead core. An experimental building with a non-traditional type of isolation system consisting of steel springs combined with viscoelastic fluid dampers was designed and built at the National Technical University of Mendoza, Argentina in 2005. This building, as well as a twin one resting on rigid foundation, was instrumented with a network of accelerometers and several near-fault earthquake records have been obtained. The analysis of these records as well as a theoretical study of the behavior of the buildings for several strong near-fault records obtained at different locations throughout the world is presented. A comparison with analytical results for the same building but with LRB instead of steel springs and dashpots is also described.

As it has been set by several authors, near-fault earthquakes have, in general, a large displacement

*Corresponding author, Professor, E-mail: mtornell@frm.utn.edu.ar

demand on isolation systems because of their acceleration pulses. These large displacements are difficult to handle in practice and should be controlled by adding damping at the isolation interface (Heaton *et al.* 1995, Makris *et al.* 1998, Mahmoud and Jankowski 2010).

Naeim *et al.* (1999) and Gavin *et al.* (2002), showed that, in order to control the large displacements caused by near fault earthquakes, it is imperative to use large damping in the isolation system. Most popular isolators like elastomeric or sliding bearings supply a limited amount of damping and therefore, the use of additional devices that provide extra damping is required. Larger damping in the isolation system effectively reduces the displacement of the isolators, but at the expenses of larger floor accelerations and story drifts. However, this is a solution for reducing isolators' displacements, which is a need for reducing dimensions and cost of the isolators. Studies in bridges also demonstrated the importance of additional damping for the displacement control in the case of near-fault earthquakes (Lee *et al.* 2004). Other authors compared the dynamic response of structures with various types of isolation systems subjected to near fault earthquakes, finding that mixed systems of elastomeric bearings and viscoelastic fluid dampers, (or frictional dampers) are an efficient alternative for controlling displacements (Mazza *et al.* 2004). Xu *et al.* (2007), studied the behavior of non linear viscoelastic fluid dampers, for near fault earthquakes. They found that when the period of the pulse is larger than the period of the structure, there is a large reduction of maximum displacements and the amount of energy that is dissipated. Another characteristic of near-fault earthquakes is their large vertical accelerations. In general, traditional isolation systems produce an amplification of the vertical accelerations instead of a reduction. Mazza and Vulcano (2004) studied the effect of the vertical accelerations on the response of base-isolated structures subjected to near-fault ground motion. They considered a five-story reinforced concrete building and concluded that, in the case of near-fault earthquakes, when the vertical component of the earthquake is taken into account, the isolators can undergo tensile loads. This effect depends on the ratio between vertical and horizontal stiffness of the isolators. The time history of the axial loads emphasized that the vertical load in the isolators is underestimated when their vertical deformability is neglected. Moroni *et al.* (1998) have reported an amplification of earthquake motion in the vertical direction in an experimental four-story reinforced concrete building isolated with high damping rubber bearings. The average vertical acceleration at roof level for several small earthquakes was twice the vertical acceleration at the same level recorded in a twin building with fixed base condition. However, the vertical amplifications recorded during the big 02-27-2010 earthquake were similar in both buildings. The use of steel spring isolators with large damping in both horizontal and vertical directions, as in the case in the GERB system, can help controlling vertical accelerations as well as isolator's displacements. Nawrotzki (2005) compared the response of the same structure subjected to 11 near fault seismic motions, for three support conditions, namely, fixed base, elastomeric bearings and steel springs combined with viscoelastic fluid dampers. He reported that both methods can be appropriate for reducing seismic demand. Vertical reactions and horizontal displacements were smaller in the case of springs combined with large viscous damping than in the case of elastomeric bearings.

A building constructed in 1990-91 on helical springs and viscoelastic fluid dampers at Santa Monica, California, was severely shaken by the 1994 Northridge earthquake, $MW = 6.7$. The structure consisted of a three-story braced-steel-frame residential building and was located at only 24 km from the epicenter. Makris and Deoscar (1996) reported the behavior of the building and developed analytical models for predicting its dynamic response.

The isolation system of this building is of the same type than the one studied here; therefore, the

conclusions of that experience are of interest. However, there are important differences between both cases. In the Santa Monica building the isolators had a total displacement capacity of only 55 mm in any direction, while in the Mendoza building, the displacement capacity is 200 mm. The ratio of vertical to horizontal stiffness of the springs was 2.8 in the first case; while in this case are 7.5 (2.7 times larger). Peak accelerations recorded at the base of Santa Monica's building were near 0.5 g in horizontal direction and 0.2 g in vertical direction. The authors concluded that horizontal displacement demand at the isolators was 53.8 mm, that is, close to the displacement capacity, and that the peak horizontal acceleration on the structure was reduced 45% by the action of the isolation system. The only damage reported were some cracks in the foundation of a steel frame that was added at the entrance of the garage of the building after construction and that was "rigidly" connected to the structure and to the ground.

This work presents the seismic response of a three story reinforced concrete residential building for university students. This building has a base isolation system that differs from traditional ones in the mechanism of energy dissipation. The isolation system consists of helical steel springs and viscoelastic fluid dampers, provided by GERB from Germany (GCS: GERB Control System, as per its English acronym). Springs provide flexibility in both horizontal and vertical directions, but are considerably more rigid in the vertical direction than in the horizontal one. Viscoelastic fluid dampers work in horizontal as well as vertical directions, supplying a large percent of critical damping. The design of the isolation system has been done taking into account the impulsive characteristic of near fault earthquakes as well as the need for controlling isolators' displacements. This study presents: (a) Analytical results for the seismic response of the building subjected to a number of near fault strong earthquakes and its comparison to the case of lead core elastomeric bearings (LRB). The response for fix base condition is also evaluated as a reference (FB). And (b) results of actual earthquakes registered at the site by a network of accelerometers installed in the isolated building as well as in the non-isolated one.

The analytical models were submitted to the three components of 17 near fault earthquakes records registered at different locations. All these records present long pulses of acceleration. The directions of the components are assumed to be along the principal directions of the building. Dynamic responses are obtained in the time domain using non-linear models and numerical integration. It is worth mentioning that the spring system was selected for two reason; (1) It was intended to test a system different from the more common LRB one and (2) It was more economical than the LRB system because GERB gave a promotional price.

The building on GCS isolators, as well as the twin one with fix-base, was instrumented with a network of accelerometers. Five small earthquakes have been recorded up to the present.

Analytical results show the advantage of the isolated structures as compared with the fix-base case; the importance of large damping for displacement control of the isolators; the influence of damping in the response of the isolated structure in terms of accelerations and inter-story drifts and the efficiency of the GCS system in controlling vertical demands.

2. Description of building with seismic isolation

The building has three stories of rectangular shape 8.00×7.60 m. It is composed by reinforced concrete slabs, columns and beams. The exterior walls are reinforced masonry and the interior partitions are plastering board panels. Foundations under seismic isolators are continuous beams.

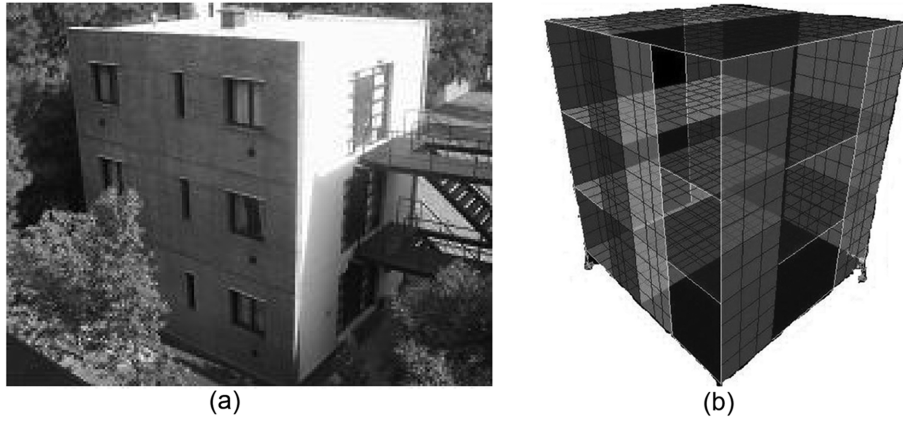


Fig. 1 General view of the building with seismic isolation: (a) general view of the building and (b) finite element model

Table 1 Masses of building for two situations

Level	Fix-base building (kg s ² /m)	Base isolated building (kg s ² /m)
0		8.962
1	6.906	6.906
2	5.633	5.633
3	4.696	4.696
Total	17.235	26.197

Fig. 1(a) shows a general view of the building and Fig. 1(b) its finite element model.

The masses considered in the analysis for the isolated as well as the fix-base cases are in Table 1. They include 25% of live loads.

Structural gaps and flexible joints were designed to allow for free horizontal and vertical displacements of the isolated building. Fig. 2(a) shows flexible joint sewer pipe and Fig. 2(b) shows



Fig. 2 Flexible joints at isolation level: (a) flexible joint for sewer pipes and (b) flexible joint for gas pipes



Fig. 3 Structural gaps and steel plate protection

flexible joint gas pipe.

Structural gaps were covered with steel plates fixed to the building and free at the other end in order to allow for horizontal and vertical displacements (Fig. 3).

All the stairs are at the exterior of the building and are not connected to it in the horizontal direction. All elements that form the isolation system (spring isolators and viscoelastic fluid dampers) are protected by a special coating that lasts for at least twenty years. Annual inspection is recommended.

Because of the high damping characteristic of the isolation system, the building has shown to be very stable under wind excitation of up to 80 km/hour.

3. Seismic isolators

Two different system of seismic isolation were considered. The first one is composed by four LRB located at each corner of the building. This system was evaluated at the design stage but was not used for the final design. Chilean code NCH2745-2003 was applied for designing the isolator's characteristics. Their final dimensions are found in Table 2. The constitutive curve of the isolators that was used for the non-linear dynamic model is shown in Fig. 4 and Table 3.

The LRBs are supposed to remain elastic in the range ± 18 mm, without energy dissipation, while the GCS isolators are always dissipative.

Table 2 Final dimension of LRB isolator

Isolator's characteristic	Value	Unit
Isolator's diameter	600	mm
Lead core diameter	150	mm
Total height	268	mm
Plate rubber thickness	8	mm
Plate steel thickness	2	mm

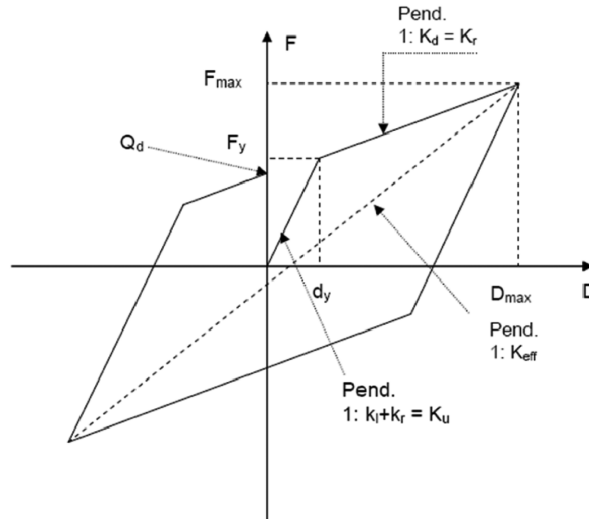


Fig. 4 Constitutive characteristic of LRB isolator

Table 3 Characteristics of LRB isolators for maximum displacement

Parameter	Notation	Value	Unit
Maximum displacement	D_{max}	417.20	mm
Postyield stiffness	K_d	736.31	kN/m
Effective total stiffness	K_{eff}^{total}	4241.70	kN/m
Vertical stiffness	K_v	5437185	kN/m
Yield displacement	d_y	18	mm
Yield force	F_y	159.08	kN
Maximum force	F_{max}	442.38	kN
Isolation building frequency	f_i	0.637	Hertz
Effective damping	ξ_{eff}	17.60	%
Characteristic strength	Q_d	135.21	kN

The natural frequency of the building with LRB isolators is 0.637 Hertz.

The other isolation system that was evaluated (the one that was finally used in the actual building design) was the GCS's. It is made of four helical steel springs packages, also located at the corners of the building, together with four viscoelastic fluid dampers. The natural frequency of the building with the GCS system is 1.00 Hertz. Steel springs have the advantage of well known behavior, stability in time, independence of temperature and having neither creep nor residual displacements. However, they have the disadvantage of low damping (2% critical), which makes it necessary to use additional devices to supplement the damping. This kind of devices are normally used for equipment isolation or for filtering vibrations produced by vehicular or railroad traffic. There are few experiences in its uses for base isolation purposes.

Since the capacity of an individual helical spring is limited to moderate loads, the use of packages of springs is required (Fig. 5(a)). Fig. 5(b) shows the viscous damper used in parallel with the spring isolator. Fig. 6 shows the location of the isolation system under the building.

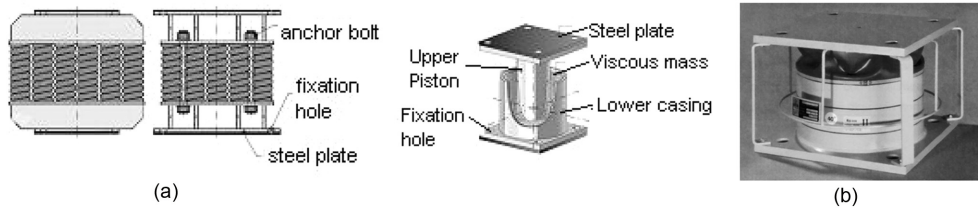


Fig. 5 (a) Packages of springs and (b) viscoelastic fluid dampers

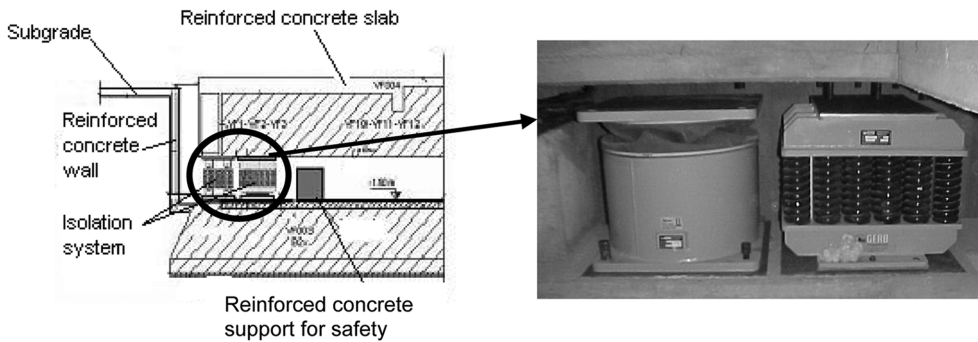


Fig. 6 Location of the isolation system under the building

Vertical and horizontal stiffness of springs can be evaluated by Eqs. (1) and (2) (Nawrotzki 2000)

$$k_v = \frac{Gd^4}{8nD^3} \tag{1}$$

$$k_H = \frac{1.13 \cdot 10^6 d^4}{nD(0.204h_s^2 + 0.256D^2)} [N \cdot m] \tag{2}$$

- Where
- G = shear modulus of steel
 - d = diameter of spring wire
 - n = number of buckles
 - D = external diameter of spring
 - h_s = free height of spring

The number of springs for isolator depends on the static and dynamic demand imposed by service and seismic loads. In the present case, due to asymmetry of loads, two isolators are composed by 30 springs, with a load capacity of 921 kN while the other two are composed by 28 springs for a force capacity of 860 kN. A summary of the characteristics of GCS used are in Table 4.

The structural systems, including the isolators, have a horizontal natural frequency of 1 Hz, and a vertical one between of 3 to 3.5 Hz. For earthquake input excitation the isolation system imposes to the structure a dynamic motion composed by vertical, horizontal, swaying and rocking. Part of the

Table 4 Characteristics of isolation system (GCS)

Parameter	Notation	Value	Unit
Nominal vertical load capacity	F_v	860-921	kN
Vertical stiffness	K_{vg}	35.400	kN/mm
Horizontal stiffness	K_h	4.730	kN/mm
Horizontal damping coefficient	c_h	26	%
Vertical damping coefficient	c_v	13	%
External diameter of spring	D_g	105	mm
Spiral diameter of spring	d_g	26	mm
Free height of spring	h_s	270	mm

horizontal excitation is transferred to swaying and rocking modes and is dissipated by the isolation system, thus reducing the seismic demands on the superstructure.

The viscous damper has an inferior container with a viscous material. A piston attached to the upper part is immersed into the viscous material generating viscous forces in three orthogonal directions. The isolation system formed by springs and viscoelastic fluid dampers, has a linear stiffness in all directions and an almost linear damping as a function of velocity.

The viscoelastic fluid dampers were designed for a peak velocity of 2 m/s and for percentages of critical damping of 26% in horizontal and 13% in vertical directions. With these values, the horizontal displacements are limited to 150-200 mm and the vertical ones to 30-50 mm, which are compatible with the displacements admitted by the springs and dashpots.

3.1 Viscoelastic fluid dampers

The GCS combines helical steel springs and viscoelastic fluid dampers. GERB fluid dampers exhibit increasing elasticity as frequency increases. Makris and Constantinou (1991) proposed a fractional-derivate Maxwell model for viscous dampers used for vibration isolation to fit the viscoelastic properties. The type of viscous damper consists of a piston moving in a highly viscous gel. The model was validated by dynamic experimental testing. The paper also presented the same analytical results for a single-degree-of-freedom viscous damper system. The fluid used in the test is a form of silicon gel with nearly temperature-independent properties in the range of $-40/-130^\circ\text{C}$, which exhibits viscoelastic behavior, namely, behavior that incorporates both elastic and viscous characteristic. The work found a fractional derivative Maxwell model to fit viscoelastic properties of a type of viscous damper. The paper defined an equivalent SDOF viscous oscillator whose response is essentially the same as that of the viscous damper isolator. They obtained a good comparison between analytically predicted and recorded force-displacement loop in tests with time-varying amplitude and frequency. The equivalent oscillator has the combined stiffness of the spring and storage stiffness of the fractional Maxwell element and the damping coefficient of the fractional Maxwell element. The storage stiffness and damping coefficient was evaluated at the fundamental frequency of the oscillator. The equivalent oscillator was found to predict well the dynamic response of the SDOF viscous damper oscillator when subjected to general dynamic loading. Further results of this approach can be seeing in Makris and Constantinou (1992).

4. Near-fault earthquakes

There are clear pieces of evidence that seismic motions near a fault have a pulse of acceleration that demands the structure a high energy input motion, just instants after the beginning of the earthquake. Several investigations point out this difference respect to earthquakes registered far away from the source (Iwan 1998, Alavi *et al.* 2001, Sasani *et al.* 2000). Near-fault earthquakes impose important horizontal displacement demands to the structure with larger inelastic displacements

Table 5 Earthquake characteristics

Earthquake	Station	Date	M	Epicentral distance km	Soil type	P_D cm-s	PGA g	PGV cm/s	PGD cm
Tabas Irán	Tabas 9101	09/16/78	7.4	3.00	C	13.20	0.85	121.40	94.60
Imperial Valley	Bond Corner	10/15/79	6.9	2.50	C	24.90	0.78	45.90	14.90
Coalinga	Transmitter Hill	07/22/83	5.7	9.20	A	4.70	1.08	39.70	5.40
Loma Prieta	Corralitos Eureka	10/17/89	7.1	5.10	B	8.40	0.64	55.20	10.90
Loma Prieta	Gatos	10/17/89	7.1	3.50	B	-	0.59	91.60	34.80
Cape Mendocino	Cape Mendocino	04/25/92	7.0	8.50	A	4.90	1.50	127.40	41.00
Cape Mendocino	Petrolia	04/25/92	7.0	-	A	8.70	0.662	89.45	25.83
Northridge	Tarzana Cedar Hill Nursery	01/17/94	6.7	17.50	B	32.40	1.78	113.60	33.20
Northridge	Rinaldi Receiving Sta	01/17/94	6.7	7.10	C	11.10	0.84	170.30	47.33
Northridge	La Country Fire Station	01/17/94	6.7	18.00	B	12.30	0.589	94.72	39.84
Northridge	Sylmar	01/17/94	6.7	18.00	B	8.50	0.842	124.70	28.91
Kobe	Kobe Observatory JMA	01/17/95	6.9	0.60	B	20.00	0.82	81.30	17.70
Chi-Chi Taiwan	TCU084	09/29/99	6.9	10.40	B	11.60	1.16	114.70	31.40
Duzce Turquía	Lamont375	11/12/99	7.3	8.20	B	7.90	0.97	36.50	7.20
Imperial Valley	El Centro Array N° 6	11/23/77	-	-	B	14.70	0.456	108.71	55.16
Caucete San Juan	INPRES	11/23/77	7.4	69.19	C	22.39	0.20	20.30	-
Las Heras Mendoza	Las Heras	01/26/85	5.9	31.00	C	10.20	0.41	28.12	3.87

P_D : Destructiveness potential factor (Araya and Saragoni 1984)

PGA: Horizontal peak ground acceleration, PGV: Horizontal peak ground velocity; PGD: Horizontal peak ground displacements

Table 6 Soil characteristics

Soil type	USGS classification	Wave shear velocity
Rock	<i>A</i>	> 750 m/s
Firm	<i>B</i>	360 á 750 m/s
Soft	<i>C y D</i>	< 360 m/s

than the ones usually computed for far-fault earthquakes (Baez *et al.* 2000).

Makris and Black (2004) investigated the importance of distinguishing between acceleration pulse and velocity pulse and identified two classes of near-source ground motion: those where the peak ground velocity is the integral of a distinguishable acceleration pulse and those where the peak ground velocity is the result of a succession of high-frequency, one-side acceleration spike. The work concluded that acceleration pulses are in general superior engineering demand parameters for most civil structures than velocity pulses. Long velocity pulses are worth considering only when the responses of very long period structures are of interest ($T_s > 4$ s.)

Therefore, seventeen earthquakes records that show similar characteristics of near-fault location, local soil conditions, and macro-seismic mechanism in the city of Mendoza, Argentina, have been selected for this study. The only seismic record that is available for the Mendoza area is the one obtained at Las Heras in 1985 (Table 5). This record has the characteristic pulse of near fault earthquakes. A list of these earthquakes with their main characteristics is in Table 5. The corresponding soil characteristics are in Table 6.

The PGV and PGD data of Table 5 are taken from PEER strong motions data base (<http://peer.berkeley.edu/smcat/process.html>) that computes velocity and displacements by frequency domain integration. It should be pointed out that these integration processes can lead to important differences respect to actual values.

5. Analytical models

A finite element time history analysis was carried out using the SAP2000 program (Fig. 1(b)) to evaluate the seismic responses. The isolators were considered non-linear and were modeled by means of special elements (Link-Support type) implemented in the program. The relation $f = kd_k + cd_c^\alpha$ is used where k is the spring stiffness, c the damping coefficient, d_k the spring displacement, \dot{d}_c the velocity of the damper and α is a coefficient that determines the non-linear characteristic of the response (Wilson 2002).

Only the LRB isolators were considered as non-linear taking into account the force-deformation (Fig. 4) (Olmos and Roesset 2010). The GCS isolation devices were modeled by means of Link-Support type element. For each direction of analysis the stiffness of springs and damping coefficient were defined.

6. Analytical results

6.1 Displacements

Due to near-fault characteristics of earthquakes, the design criterion for the isolation system was

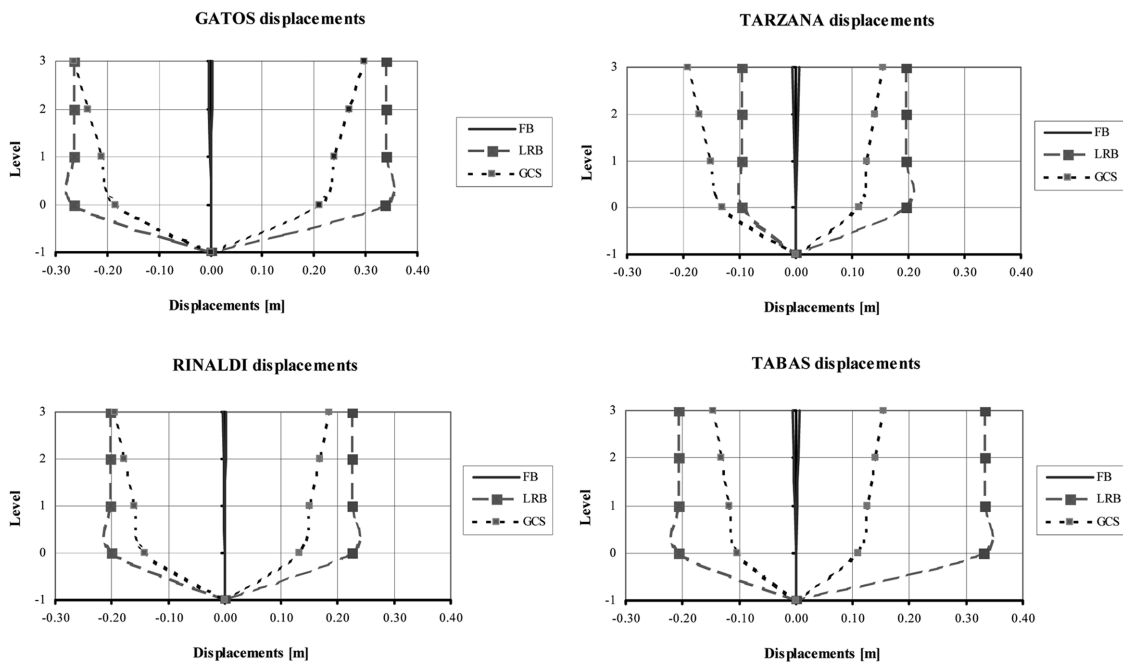


Fig. 7 Horizontal displacements for three different support conditions FB, LRB bearings and GCS isolation (levels 0: above isolators; level -1: ground level)

displacement control. Several situations were considered and the dynamic response was computed for displacements, inter-story displacements, base shear and elements internal forces. Fig. 7 shows the horizontal displacements at different building levels for four representative earthquakes.

Three different support conditions were investigated: FB, LRB bearings and GCS isolation system. The maximum positive and negative displacements have been plotted in each of the four levels. Vertical and horizontal displacements at the isolation system for the complete set of earthquakes are in Table 7.

The relative displacement with respect to the ground can see in Fig. 8.

For FB condition the maximum displacement at the roof is 1.91 cm (Cape Mendocino), that is, 0.25% of the building height. For the LRB case, the larger displacements are at the isolation level and remain almost constant with height. The largest displacement at top of the building is 47.2 cm (Sylmar). For the GCS system the largest displacements are at the isolation level but, differing from the LRB case, are substantially incremented with height. This occurs because the vertical flexibility of springs induces rocking motion that amplifies the horizontal displacements with height. The largest roof displacement for this case is 33.4 cm (Kobe). It can be observed that the maximum for the different base conditions are for different earthquakes. The presence of large pulses in the seisms of Table 5 can explain why the displacements obtained for some earthquakes (Cape Mendocino, Tarzana and Kobe) present asymmetries, tending to respond almost exclusively in one direction. The presence of larger vertical, swaying and rocking motions of the GCS system as compared with the LRB case is apparent.

Inter-story drifts for FB, LRB and GCS cases are displayed in Fig. 8. LRB and GCS cases were corrected by eliminating rigid body motions of building above base isolation. For FB, the maximum

Table 7 Vertical and horizontal displacements at the isolation system

Earthquake	LRB		GCS	
	$U_{max.}$ (Horizontal) (cm)	$U_{max.}$ (Vertical) (cm)	$U_{max.}$ (Horizontal) (cm)	$U_{max.}$ (Vertical) (cm)
Tabas	33.20	0.0626	18.92	6.30
Imperial Valley	9.30	0.0790	15.68	5.75
Coalinga	6.90	0.0439	14.01	4.20
Corralitos	9.57	0.0507	9.05	4.20
Los Gatos	33.86	0.0644	21.04	6.40
Cape Mendocino	24.36	0.0567	14.20	5.35
Tarzana	27.22	0.0728	13.10	7.70
Rinaldi	33.36	0.0686	19.25	4.20
Kobe	15.06	0.0451	28.15	5.65
Taiwan	43.52	0.0541	18.40	6.25
Duzce	3.70	0.0421	2.30	3.30
Petrolia	21.42	0.0120	15.54	2.71
New Hall	44.80	0.0478	18.91	5.76
Sylmar	44.97	0.0517	14.40	2.69
El Centro	18.43	0.1061	11.69	2.15
Caucete	6.80	0.0097	3.40	0.85
Mendoza-85	4.69	0.0062	2.90	0.567

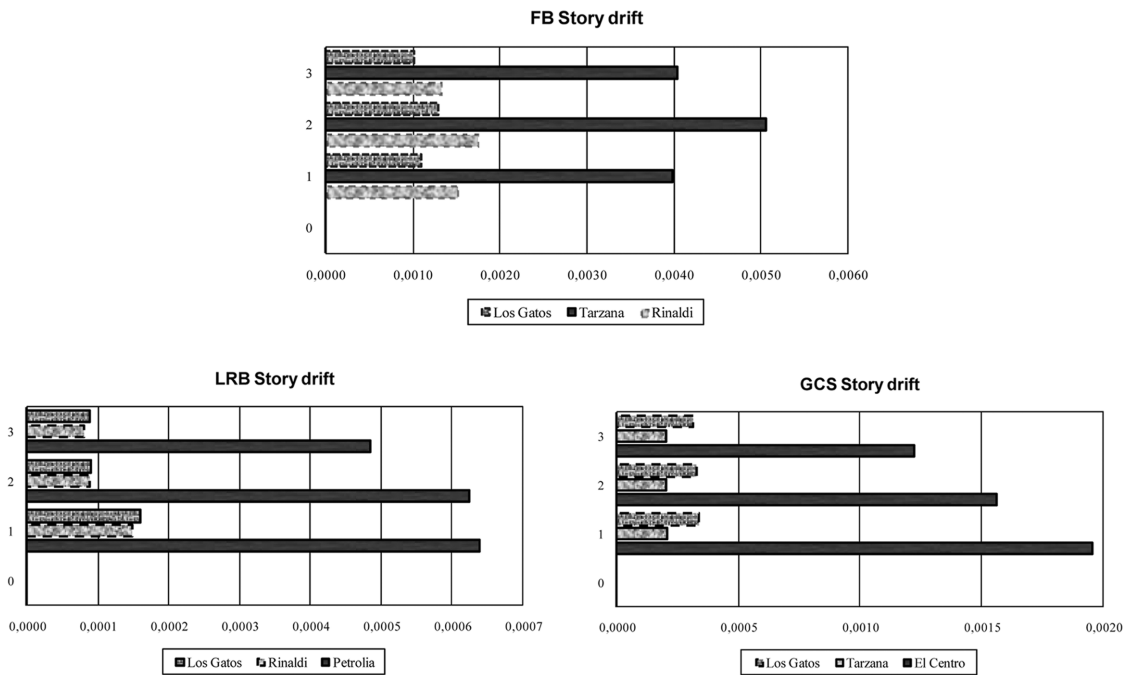


Fig. 8 Story drifts for three different support conditions FB, LRB bearings and GCS isolation

inter-story drift is 0.0051 (Tarzana). The maximum drift for the LRB case is 0.00064 (Petrolia), that is, 11% of the FB case. For the GCS case, the maximum drift was 0.00196 (El Centro), that is, 38.5% of the rigid case.

As it was mentioned, LRB isolators were not used in practice. However, for evaluation purpose they were considered bolted to foundation and superstructure.

6.2 Accelerations

Fig. 9 shows accelerations for FB, LRB and GCS isolation systems for four of the earthquakes of Table 5. The maximum positive and negative acceleration are plotted for each of the four levels. For the FB condition there is an amplification of horizontal peak accelerations from ground level to roof level between 8% (Taiwan) to 435% (Coalinga). Vertical accelerations are amplified from 4%

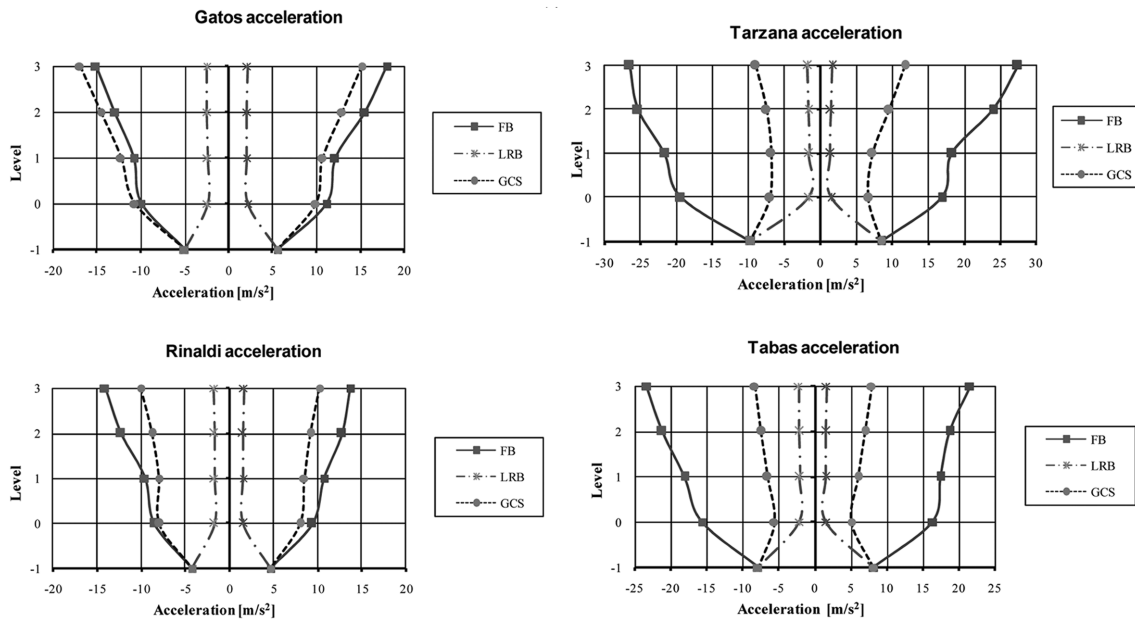


Fig. 9 Horizontal acceleration for three different support conditions FB, LRB bearings and GCS isolation (levels 0: above isolators; level -1: ground level)

Table 8 Vertical acceleration for FB condition

Level	Imperial Valley		Kobe		Petrolia	
	$\ddot{U}_{v_{min}}$	$\ddot{U}_{v_{max}}$	$\ddot{U}_{v_{min}}$	$\ddot{U}_{v_{max}}$	$\ddot{U}_{v_{min}}$	$\ddot{U}_{v_{max}}$
	[m/s ²]		[m/s ²]		[m/s ²]	
3	-6,6766	4,4693	-3,0767	3,4613	-2,5184	2,5162
2	-6,1428	4,1974	-3,0517	3,4298	-2,4186	2,4874
1	-5,0075	3,4913	-3,0529	3,3425	-1,9219	2,2357
0	-3,6570	2,8971	-3,1611	3,3327	-1,2238	1,5973

Note: 0: ground level

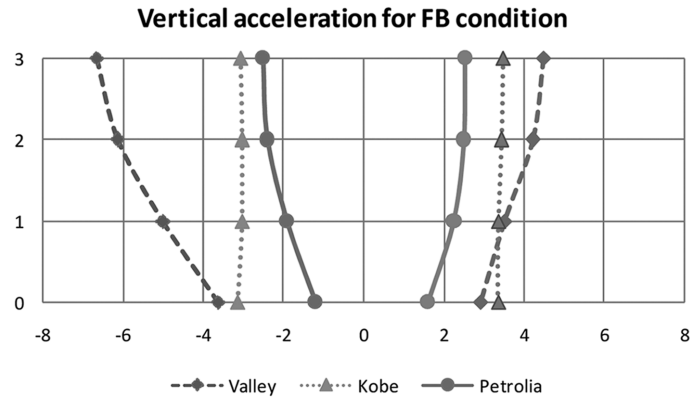


Fig. 10 Vertical acceleration for FB condition for earthquakes

(Kobe) to 106% (Petrolia). These results are indicated in Table 8. The maximum positive and negative vertical accelerations are plotted in Fig. 10.

The responses of both fixe-base building and building with LRB system were compared. The horizontal accelerations at roof level are between 92.5% (for Cape Mendocino) and 5% (for Petrolia) of the ground values. Horizontal accelerations remain almost constant with height. However, there are three earthquakes that produce amplification of accelerations between ground and roof: Northridge-New Hall (58%), Northridge-Sylmar (55%) and Imperial Valley-El Centro (29%). Vertical accelerations are incremented in all cases between 2.5% (Tabas) and 84% (Loma Prieta-Los Gatos). Maximum positive and negative horizontal accelerations for these cases are indicated in Table 9 and Fig. 11.

In GCS'case, horizontal accelerations are quite variable. There are reductions of horizontal accelerations between ground and roof to 11.50% (Loma Prieta-Los Gatos) and 80% (Cape Mendocino). However, at the same time, horizontal accelerations are increased between 56% (Northridge-Sylmar) and 176% (Tabas). Regarding vertical accelerations, the situation is also erratic. There are reductions between 2% (Coalinga) and 182% (Imperial Valley-El Centro) and increments between 19% (Imperial Valley-Bond Corner) and 226% (Cape Mendocino-Petrolia).

Thus, LRB system is more efficient than GCS for controlling horizontal accelerations, while the second is more efficient for controlling vertical accelerations. In both cases the situation for horizontal accelerations is better than for the FB case.

Table 9 Amplification of horizontal accelerations for building with LRB systems

Level	Northridge-New Hall		Northridge-Sylmar		Imperial Valley-El Centro	
	\ddot{U}_{min}	\ddot{U}_{max}	\ddot{U}_{min}	\ddot{U}_{max}	\ddot{U}_{min}	\ddot{U}_{max}
	[m/s ²]		[m/s ²]		[m/s ²]	
3	-8,58915	7,7535	-8,9519	8,5636	-4,3065	4,2042
2	-8,54414	7,7113	-8,9284	8,5106	3,9765	2,5138
1	-8,51093	7,6786	-8,9068	8,5018	3,8104	2,2301
0	-8,44884	7,6547	-8,8873	8,4475	4,8733	3,7090
-1	-5,41569	5,78193	-5,78034	8,2676	4,2809	3,254

(Level 0: Above isolators; Level -1: ground level)

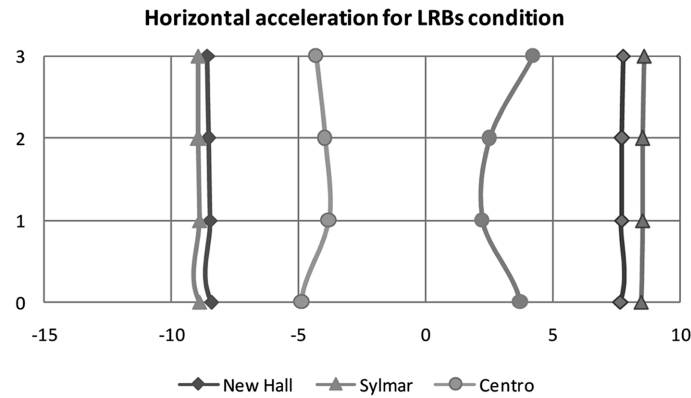


Fig. 11 Horizontal acceleration LRB condition, for three earthquakes selected

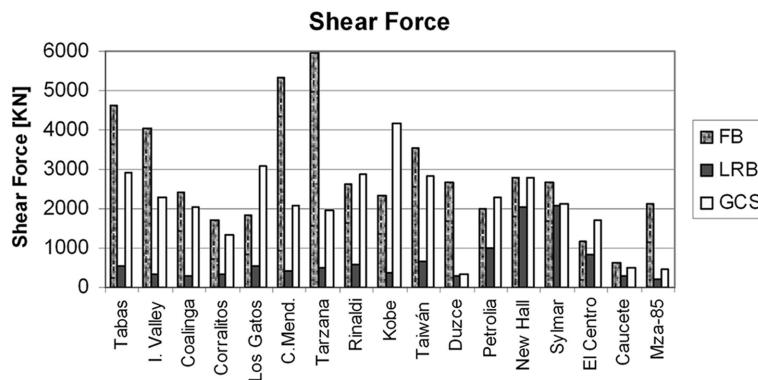


Fig. 12 Maximum base shear force for three different support conditions: FB, LRB and GCS

One of the main objectives of seismic isolation is to improve the building structural response. In general, vertical acceleration is not a problem in buildings, because their structure is designed to support vertical dead loads and live loads. However, their effect on equipments and secondary systems may be important (Wolff and Constantinou 2004).

6.3 Shear forces

Maximum base shear forces are summarized in Fig. 12. Base isolated buildings with either LRB or GCS always show lower values than for FB condition.

6.4 Base vertical reactions

The total vertical reactions for the three models are summarized in Fig. 13. For the building isolated with LRB bearings, amplification is observed for all earthquakes. However, in the case of GCS system, for most earthquakes there is a reduction, which for El Centro is 38%. The increase in vertical reaction will affect the design of the isolators' structure but will not represent a serious problem in general.

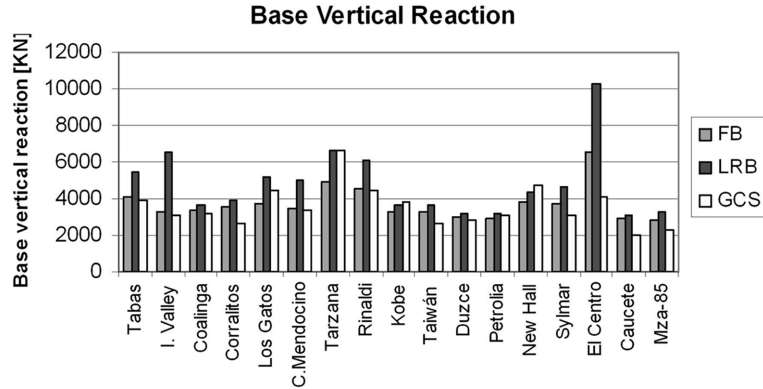


Fig. 13 Base vertical reaction for three different support conditions FB, LRB bearings and GCS isolation

6.5 Horizontal deformations of the isolation system

The relationships between relative displacement and force at the isolation system have been plotted in Fig. 14 for the case of LRB bearings for four representative earthquake records. The non-linearity of the response is apparent. There is a large incursion in the non-linear range for a few cycles, reaching a maximum of 46.7 cm for Northridge-Sylmar (for a corresponding force of 2078 kN). This result confirms the fact that the presence of long pulses of acceleration ends up with very large demands of displacements at the isolation system. In general, the need of physical space for absorbing these large displacements is not a problem for new constructions. However, in this case there were limitations due to the small space available at the site, and because of the small size of the rubber isolators needed for obtaining the design natural period.

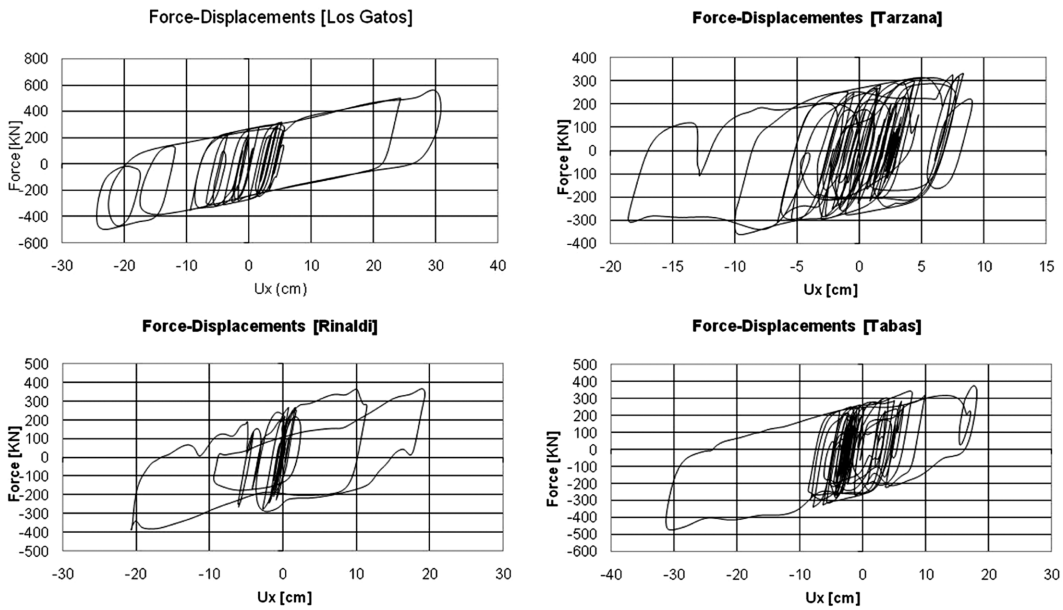


Fig. 14 Relations between relative displacement and force for the LRB bearings isolation

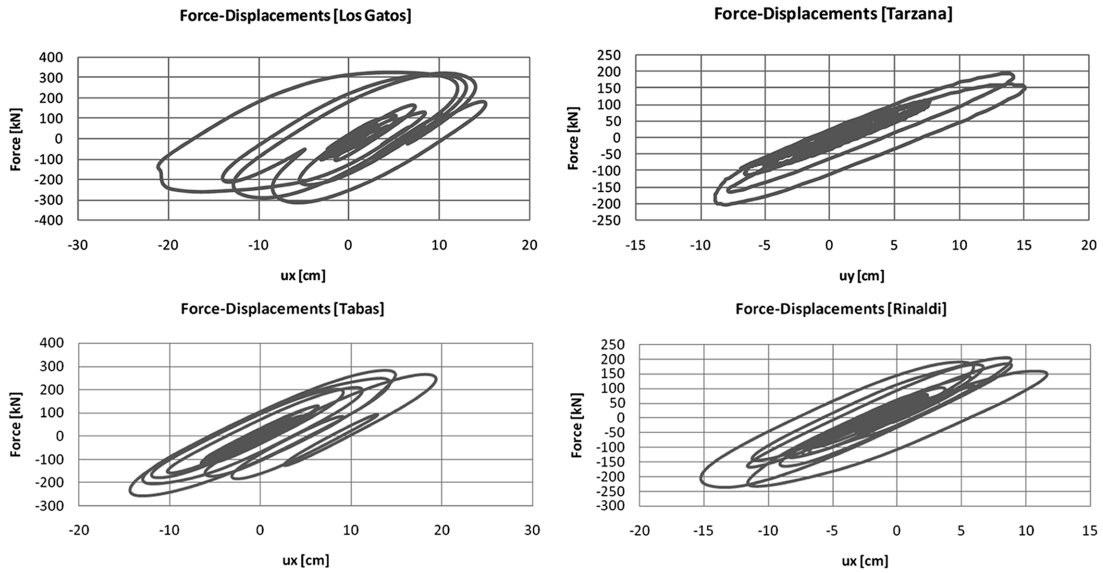


Fig. 15 Relations between relative displacement and force for the GCS isolation system

Fig. 15 shows the force-displacement relationships in the case of GCS isolators, for the same earthquakes. In this case the maximum displacement is only 28 cm, but the corresponding force has increased to 4147 kN (for Kobe earthquake).

6.6 Relationships between horizontal and vertical deformations

Figs. 16 and 17 show relationships between horizontal and vertical displacement for the LRB and

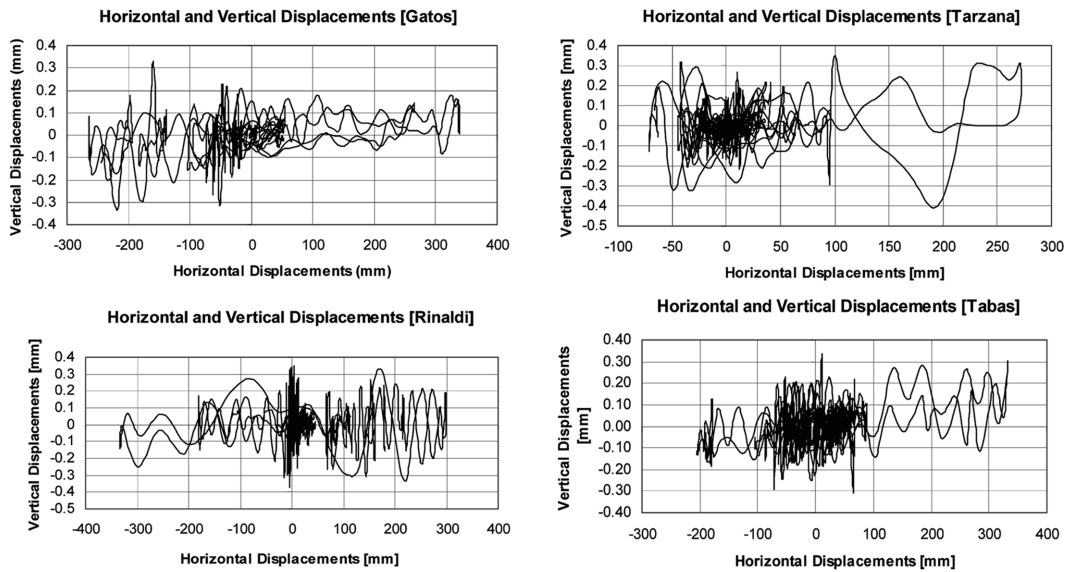


Fig. 16 Relationships between horizontal and vertical displacements LRB case

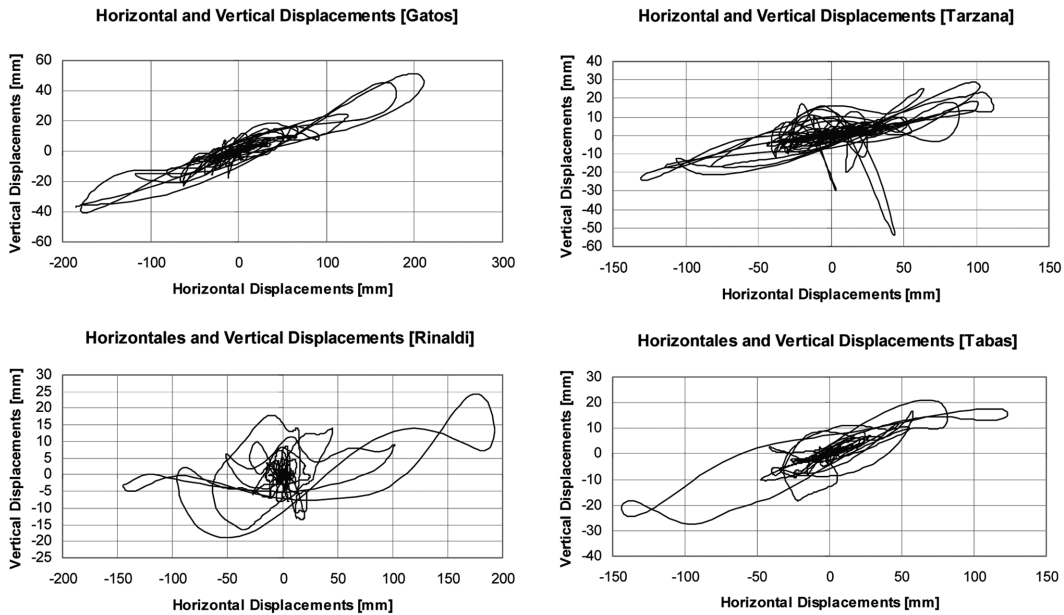


Fig. 17 Relationships between horizontal and vertical displacements GCS case

GCS cases, respectively. The advantage of this representation is that it gives some information about the coupling of vertical and horizontal displacement (Nawrotzki 2001). This graphic is useful when vertical displacements are important, like in the case of GCS system.

6.7 Maximum accelerations and displacements as a function of damping

The amount of damping in the GCS system can be changed by modifying the number of damping cylinders. Thus, it is of interest to know the optimal amount of damping for reducing the peak acceleration or peak displacement at the top of the superstructure. Jangid and Kelly (2001) showed the variation of the peak average superstructure absolute acceleration and bearing displacement against the bearing damping ratio. The response was plotted for different combinations of time periods and for a damping ratio between 0.0-0.70. The works concluded that there is a value of damping for which the superstructure acceleration of a given structural system attains a minimum

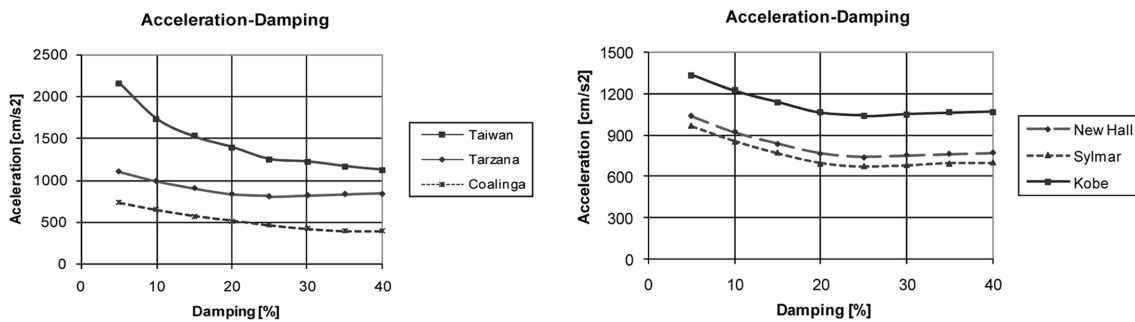


Fig. 18 Relationships between acceleration and critical damping

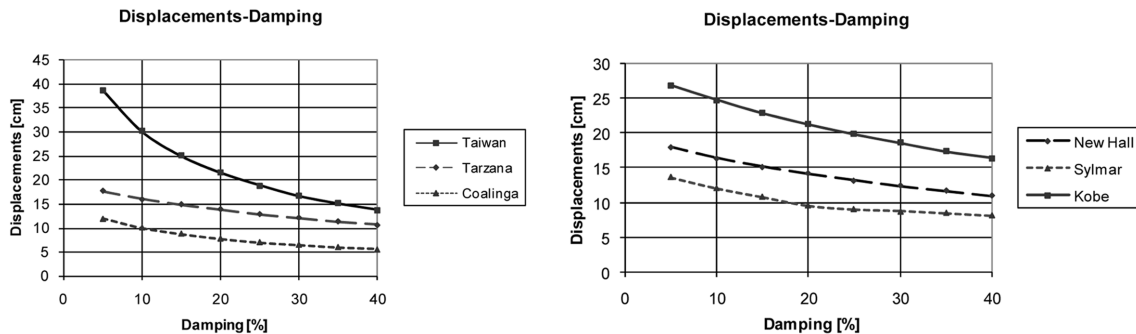


Fig. 19 Relationships between displacements and critical damping

value under ground motion however, the bearing displacement decreases with the increase in the damping.

Figs. 18 and 19 show these two quantities as a function of percentage of critical damping between to 0-60%. From the first of these figures it is clear that in this case the optimal damping is around 25% of critical. In general larger damping does not help in reducing peak acceleration, and even it could be prejudicial. As for the displacements, they always decrease with increasing damping, but over 25% the reduction is not significant.

7. Experimental results

The isolated building is instrumented with a network of accelerometers, four above GCS system and three at the roof. The fixed base building is located five meter apart from the isolated building and it is instrumented with one accelerometer at the roof that has recorded three events.

The instruments are Kinematics accelerometers, Altus K2 model, with triaxial internal sensor. The Altus K2 is a central data acquisition that also has nine external channels for acceleration recording. Thus, the network is capable of obtaining twelve acceleration records simultaneously. The network is completed with another accelerometer located at the structures laboratory (50 meters from the isolation building), which acts as free-field station.



Fig. 20 External accelerometers with metal protection

Table 10 Characteristics of main recorded earthquakes

Date	PGA [%g]	PGV [cm/s]	PGD [cm]
09-09-2005	1.60	0.681	0.102
05-09-2006	1.10	0.497	0.054
08-05-2006	12.40	3.85	0.433
09-15-2007	5.50	1.32	0.057
10-16-2008	4.50	1.46	0.054

The accelerometers are protected by a double wall metal cover, filled with polystyrene to control thermal gradients (Fig. 20).

Since the building was concluded, 40 minor earthquakes have been recorded but only five can be considered relevant. Table 10 contains the relevant characteristics of the five earthquakes.

Fig. 21 shows the change of accelerations in the three components of the earthquakes (east-west,

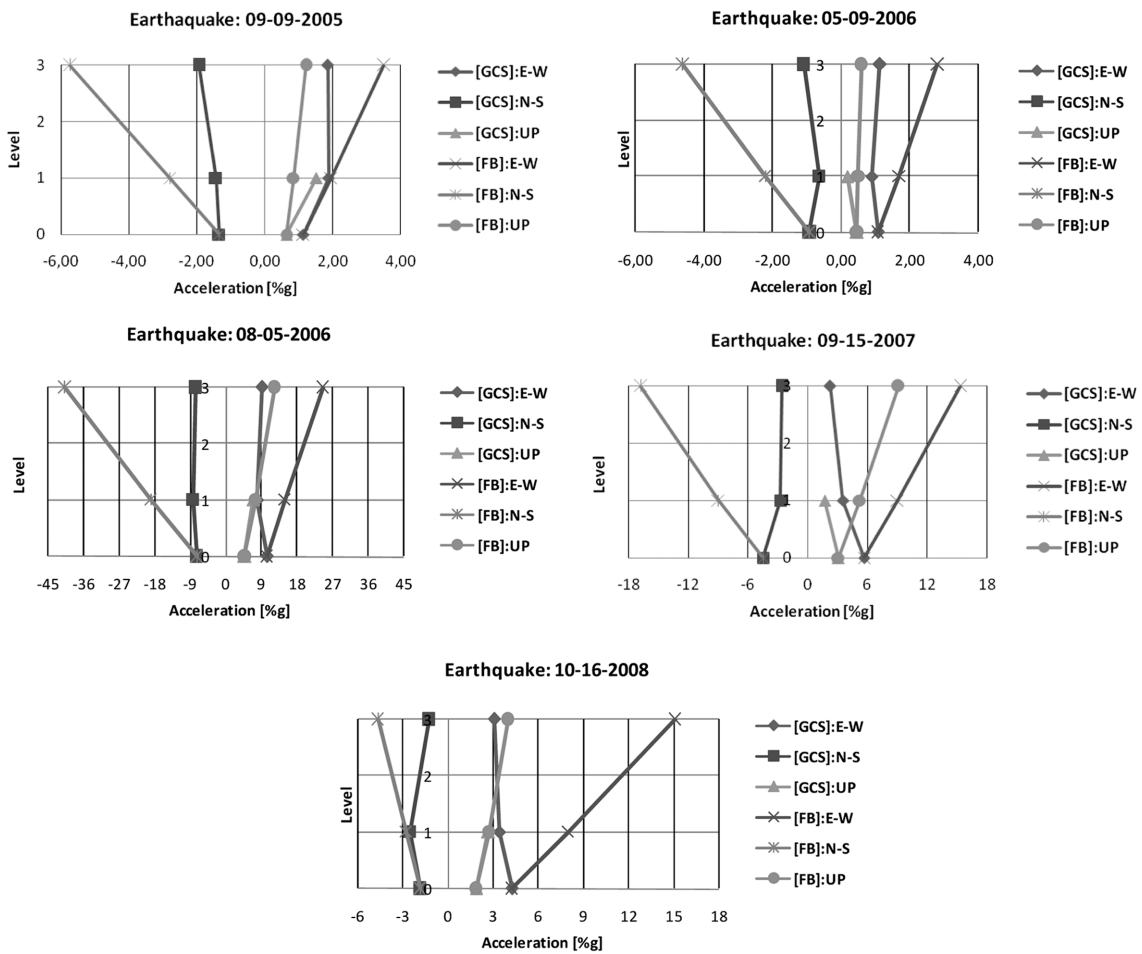


Fig. 21 Recorded acceleration for two different support conditions FB and GCS isolation

Table 11 Recorded horizontal and vertical displacements

Date	Fixed base: Roof horizontal displacements (mm)	Isolated building: Roof horizontal displacements (mm)	Isolated building: GCS horizontal displacements (mm)	Isolated building: GCS vertical displacements (mm)
09-09-2005	1.22	1.61	1.19	0.50
05-09-2006	0.65	1.00	0.73	0.25
08-05-2006	5.62	9.41	5.16	2.26
09-15-2007	1.81	0.78	0.43	0.17
10-16-2008	1.17	0.90	0.57	0.37

Table 12 Maximum GCS and fixed base story drift

Date	Fixed base: Maximum story drift	Isolated building: Maximum story drift
09-09-2005	0.0145	0.0075
05-09-2006	0.0077	0.0048
08-05-2006	0.0669	0.0076
09-15-2007	0.0215	0.0062
10-16-2008	0.0203	0.0059

north-south and vertical) for both the isolated building as well as the fixed base one. In all cases the accelerations in the isolated buildings are lower than in the fixed base case.

Table 11 shows the maximum horizontal displacements measured at roof level for two conditions: isolated building and fixed base building. Peak vertical displacements at level of the GCS system are indicated in the last column.

The maximum horizontal displacements at roof level of the isolated building are greater than in the fixed base building, with the exception of two cases. It is possible to see the pendulous effect of the movement by comparing the horizontal displacements of the isolated building, at level of the GCS isolation and the horizontal displacement at the roof. The maximum vertical displacements measured are small (less than 3 mm).

Table 12 shows the maximum values of inter-story drifts for two conditions, evaluated from the information of Table 10. The results indicate that the inter-story drifts of the isolated building are lower than those calculated for the fixed base building.

8. Conclusions

An analytical study of a three story building supported on helical steel springs and viscoelastic fluid dampers, subjected to near-fault earthquakes is presented. The same building but with lead core elastomeric bearings, LRB, is also analyzed. Both cases are compared with the response of the building for a fix-base condition. It is demonstrated that both systems present benefits with respect to the fixed base situation. With the GCS system a larger reduction of vertical acceleration can be obtained. Results show that the building with either type of isolation systems behaves better than the FB case. The presence of large acceleration pulses, characteristic of near fault earthquakes, produces very important displacements in the LRB isolators. In this particular case, the LRB could

not support very large displacements because of the reduced size that was required in order to get a reasonable natural period. There was also a physical limitation in space at the site. On the contrary, in the case of the GCS, it was easy to get large damping that could control the displacement demand.

The larger damping ratios that can be supplied by the GCS devices allow limiting the total displacements to admissible values. The dimensions of the area available for the installation of the isolated building were limited. Therefore, it was necessary to reduce the horizontal displacements. In fact, compared to LRB system, the GCS system leads to a smaller isolation drift, which means a smaller lateral displacement of the isolation system and the structure, but the floor accelerations and base shear increase.

It has been verified that the mechanism of energy dissipation of the GCS system is quite different from the LRB one, which is more frequently used for base isolation. In this particular case, because of the reduced mass of the building, LRBs resulted in relatively small natural period and normal damping values and it was not possible to get the large displacement capacity that was necessary for near fault earthquakes. The GCS system could provide enough damping to control displacements to admissible values for the available space.

With respect to displacements, in the case of LRB isolators they are concentrated at the base and are almost constant with height. In the case of GCS system, the displacements are also concentrated at the isolation level, but are not constant with height due to the presence of swaying and rocking modes of vibrations of the structure. Due to the relation between horizontal and vertical frequencies, the mechanism of energy dissipation implies horizontal as well as vertical and rotational modes. This differs substantially from the LRB systems where the energy is dissipated almost exclusively through horizontal motion.

Inter-story drifts at different levels are substantially reduced by the isolation systems. In the case of GCS, the rotational rigid motion of the building must be considered in order to get net inter-story deformations.

As in other investigations (Bozzo and Barbat 2000, Nawrotzki 2000, 2001), important increments in both horizontal and vertical accelerations with height can be observed for the FB case. On the contrary, for the LRB case there are important reductions in horizontal accelerations. These reductions are concentrated at the isolators' level and remain practically constant with height. However, for some of the earthquakes considered, there is an amplification of accelerations at the roof level, which indicates that for near fault earthquakes the response is very sensitive to the characteristics of individual motions.

For the GCS case the acceleration response is somewhat random. Important to moderate reductions between foundation and roof are obtained for some of the quakes, but there are moderate increments in others. The same is observed for vertical accelerations. This again shows the sensitivity of response to the characteristics of the earthquakes.

Base shear forces are reduced for both LRB and GCS systems, compared with FB case. The LRB system presents less shear forces than the GCS one, but larger displacements.

Vertical forces are reduced only in the GCS case, as compared with the FB case. The flexibility and high damping in the vertical direction allows this reduction. This is important for near fault earthquakes because the vertical motion is as important as the horizontal one.

In the LRB case, force-displacement relation shows a large degree of non-linearity. However the incursion in the non-linear range happens only for a few pulses of acceleration. Long pulses, a characteristic of near fault motions, means also large demands of displacement for the isolation

system, situation which is difficult to handle. GCS isolators, on the contrary, remain always linear and the displacements are controlled by high viscous damping.

Maximum vertical displacements for the LRB case are very small, close to 1.0 mm. (El Centro), while for the GCS case is of the order of 77 mm. (Tarzana record). If the two horizontal components are considered, the maximum displacement in each direction occurs at different instants, but in general the maximum in one direction has a small associate displacement in the perpendicular one. The effect of isolation damping in the building response is that maximum acceleration are reduced with increasing damping, but there is a value of damping (between 20% and 25%) after which peak acceleration increases instead of reducing.

Analytical responses to seismic records as well as experimental results indicate that, in all cases, the accelerations in the isolated building are lower than those of the building with fixed base. Maximum horizontal displacements at roof level in the isolated building are larger than in the fixed-base one (except for two cases). Maximum vertical displacements are smaller than 3 mm. Inter-story drifts of isolated building are lower than those calculated for the fixe-base building.

In general the energy dissipation mechanism of the GCS system differs from the LRB one allowing a better control of displacement demands for near source earthquakes. The spring-high damping isolation systems are a valid and economical alternative to the traditional rubber bearings for small size buildings. It is also concluded that the analytical non-linear dynamic models gives acceptable results for the response of this kind of buildings.

Seismic records of five earthquakes registered by the accelerometers' network were presented. Results indicate that the accelerations in the isolated building are lower than fixed-base building (Fig. 20). Accelerations recorded above the GCS devices are slightly lower than the accelerations recorded at free field. Experimental result indicates that the inter-story drifts in the isolated building are considerably smaller than in the case of the fixed-base building (Tables 11 and 12).

Acknowledgments

The authors wish to express their appreciation to the National Technical University, Mendoza, Argentina, to the University of Chile, Santiago, Chile, to GERB and to FONDECYT research fund (Project N° 1061265) for their financial support.

References

- Alavi, B. and Krawinkler, H. (2001), "Effects of near-field ground motion on building structures", *CUREE Publication N° CKIII-02. CUREE-Kajima Joint. Research Program, Phase II.*
- Baez, J.I. and Miranda, E. (2000). "Amplification factors to estimate inelastic displacement demands for the design of structures in the near field", *12th World Conference in Earthquake Engineering. Paper N° 1561*, New Zealand Society for Earthquake Engineering.
- Bozzo, L.M. and Barbat, A.H. (2000), *Diseño sismorresistente de edificios: Técnicas convencionales y Avanzadas*, Reverté, Barcelona, España.
- Gavin, H. and Alhan, C. (2002), "Inter-story drift amplification and damping in passive isolation systems", *00212 Seventh U.S. National Conference on Earthquake Engineering (7NCEE), Earthq. Eng. Res. Inst. (EERI)*, Boston Massachusetts.
- Heaton, T.H., Hall, J.F., Wald, D.J. and Halling, M.W. (1995), "Response of high-rise and base-isolated building

- in a hypothetical Mw 7.0 blind trust earthquake”, *Sci.*, 267:206 a 211.
- Iwan, W.D. (1998), “Evaluation of the effects of near-source ground motions” [on line], *PG&E PEER, Directed Studies Program, Berkeley*, [Available in <http://peer.berkeley.edu/news/1998may/nsource.html>].
- Jangid, R.S. and Kelly, J.M. (2001), “Base isolation for near-fault motions”, *Earthq. Eng. Struct. D.*, **30**(5), 691-707.
- Lee, T.Y. and Kawashima, K. (2004), “Effectiveness of supplementary dampers for isolated bridges under strong near-field ground motions”, *13th World Conference on Earthquake Engineering*, Vancouver. B.C., Canadá.
- Makris, N. and Black, C. (2004), “Evaluation of peak ground velocity as a good intensity measure for near-source ground motions”, *J. Eng. Mech.-ASCE*, **130**(9), 1032-1044.
- Makris, N. and Constantinou, C.M. (1991), “Fractional-derivative maxwell model for viscous damper”, *J. Struct. Eng.*, **117**(9), 2708-2724.
- Makris, N. and Deoscar, H. (1996), “Prediction of observed response of base-isolated structure”, *J. Struct. Eng.*, **112**(5), 485-493.
- Makris, N. and Chang, S. (1998), “Effect of damping mechanisms on the response of seismically isolated structures”, *Pac. Earthq. Eng. Res. Cent. (PEER)*, **1**, 146-152.
- Mazza, F. and Vulcano, A. (2004), “Base isolation techniques for the seismic protection of RC framed structures subjected to near-fault ground motions”, *13th World Conference on Earthquake Engineering, Vancouver. B.C., Canadá*.
- Mazza, F. and Vulcano, A. (2004), “Effect of the vertical acceleration on the response of base-isolated structures subjected to near-fault ground motions”, *13th World Conference on Earthquake Engineering, Vancouver, B.C., Canada*.
- Moroni, M., Sarrazin, M. and Boroschek, R. (1998), “Experiments on a base isolated buildings in Santiago, Chile”, *Eng. Struct.*, **20**(8), 720-725.
- Naeim, F. and Kelly, J.M. (1999), *Design of seismic isolated structures*, John Wiley & Sons, Inc. Printed in the United States of America.
- Nawrotzki, P. (2000), “Some strategies for the reduction of seismic structural response”, *The First International Conference on Structural Stability and Dynamics*, Taipei, Taiwan.
- Nawrotzki, P. (2001), “Seismic protection of structures by viscoelastic elements”, *The Eighth East Asia-Pacific Conference on Structural Engineering and Construction*, Nanyang Technological University, Singapore.
- Nawrotzki, P. (2005), “Visco-elastic device for the seismic control of machinery, equipment and buildings”, *9th World Seminar on Seismic Isolation, Energy Dissipation and Active Vibration Control of Structure*, Kobe, Japan.
- NCh2745 (2003), “Chilean code”, *Análisis y Diseño de Edificios con Aislamiento sísmico*, Requisitos.
- Olmos, B.A. and Roesset, J.M. (2010), “Effects of the nonlinear behaviour of lead-rubber bearing on the seismic response of bridges”, *Earthq. Struct.*, **1**(2), 215-230.
- “Processing procedure PEER strong motion data base” [on line], [available in <http://peer.berkeley.edu/smcat/process.html>].
- Sasani, M. and Bertero, V. (2000), “Importance of severe pulse-type ground motions in performance based engineering: historical and critical review”, *12th Conference on Earthquake on Engineering*, New Zealand.
- Mahmoud, S. and Jankowski, R. (2010), “Pounding-involved response of isolated and non-isolated buildings under earthquake excitation”, *Earthq. Struct.*, **1**(3), 231-252.
- Wilson, E.L. (2002), *Three dimensional static and dynamic analysis of structures, A Physical approach with emphasis on Earthquake Engineering*, CSI, Computer & Structures Inc. SAP 90, SAP2000, SAFE, FLOOR and ETABS.
- Wolff, E. and Constantinou, M.C. (2004), “Experimental study of seismic isolation systems with emphasis on secondary system response and verification of accuracy or dynamic response history analysis methods”, *Technical Report MCRRT-04-001*, University at Buffalo, State University of New York. Department of Civil, Structural and Environmental Engineering.
- Xu, Z., Arawal, A.K., He, W.L. and Tan, P. (2007), “Performance of passive energy dissipation systems during nearfield ground motion type pulses”, *Eng. Struct.*, **29**(2), 224-236.

List of symbols

ξ_{eff}	Effective damping LRB isolator
c	Damping coefficient
c_h	Horizontal damping coefficient GCS isolator
c_v	Vertical damping coefficient GCS isolator
d	Diameter of spring bar
d_g	Spiral diameter of spring
d_c	Velocity of the damper
d_k	Spring displacements
d_y	Yield displacement LRB isolator
D	Maximum displacement LRB isolator
D_g	External diameter of spring
f	Isolator force
f_i	Building frequency with LRB isolation
f_v	Frequency GCS system
f_{ri}	Frequency GCS system with lower rotation center
f_{rs}	Frequency GCS system with upper rotation center
F_{max}	Maximum force LRB isolator
F_v	Nominal load vertical capacity GCS isolator
F_y	Yield force LRB isolator
G	Shear modulus of steel
h_s	Free height of spring
k	Spring stiffness
K_d	Postyield stiffness LRB isolator
K_{eff}^{total}	Effective total stiffness LRB isolator
K_h	Horizontal stiffness GCS isolator
K_v	Vertical stiffness LRB isolator
K_{vg}	Vertical stiffness GCS isolator
M	Richter magnitude
n	Number of buckles
P_D	Destructive potential
PGA	Horizontal peak ground acceleration
PGV	Horizontal peak ground velocity
PGD	Horizontal peak ground displacement
Pm_i	Pendulum mode with lower rotation center in GCS system
Pm_s	Pendulum mode with upper rotation center in GCS system
Q_d	Characteristic strength LRB isolator
r_s	Distance of lower rotation center in GCS system
r_i	Distance of upper rotation center in GCS system
T	Response time
T_h	Period of building with GCS isolation
T_m	Torsion mode GCS system
ux	Horizontal displacements in X

uy	Horizontal displacements in Y
$U_{\max.(\text{Horizontal})}$	Maximum horizontal displacement at the isolation system
$U_{\max.(\text{Vertical})}$	Maximum vertical displacement at the isolation system
U_{\min}	Minimum vertical acceleration for FB condition
U_{\max}	Maximum vertical acceleration for FB condition
\ddot{U}_{\min}	Negative horizontal acceleration with LRB system
\ddot{U}_{\max}	Positive horizontal acceleration with LRB system
V_m	Vertical mode GCS systems